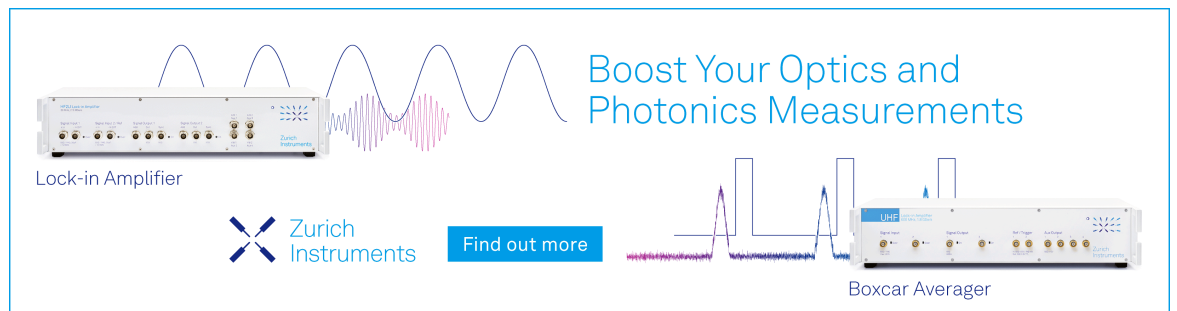# Stochastic simulation of hydrogen–oxygen auto-ignition at the microscale ⊘

C. Yang [ID] ; Y. Hu [ID] ; X. Y. Wang [ID] ; Q. Z. Hong [ID] ; Q. H. Sun ✉ [ID]

Check for updates

View Online

Export Citation

Stochastic simulation of hydrogen–oxygen auto-ignition at the microscale

View Online   Export Citation   CrossMark

C. Yang,[1] [iD] Y. Hu,[2] [iD] X. Y. Wang,[2] [iD] Q. Z. Hong,[2] [iD] and Q. H. Sun[2,3,a] [iD]

AFFILIATIONS

[1] Wide Range Flight Engineering Science and Applications Centers, Institute of Mechanics, Chinese Academy of Sciences, Beijing 100190, China
[2] State Key Laboratory of High Temperature Gas Dynamics, Institute of Mechanics, Chinese Academy of Sciences, Beijing 100190, China
[3] School of Engineering Science, University of Chinese Academy of Sciences, Beijing 100190, China

[a] Author to whom correspondence should be addressed: qsun@imech.ac.cn

ABSTRACT

A hybrid stochastic simulation method is developed to study H_2–O_2 auto-ignition at the microscale. Simulation results show that the discrete and stochastic characteristics of reaction collisions have notable impacts on the ignition process, particularly in the early stages when only a few radicals exist. The statistical properties of ignition delay time, which reflect the accumulated stochasticity during ignition, are obtained and analyzed for different initial temperatures and total molecular numbers. It is found that the average and standard deviation of ignition delay time increase as the total molecular number decreases, with this phenomenon being particularly pronounced near the crossover temperature. When the total molecular number is sufficiently small, the chain initiation reaction becomes crucial to the stochastic properties, as its average firing time exhibits an inverse proportionality to the total molecular number. As the total molecular number increases, the influence of other chain reactions intensifies, causing the power law relation between standard deviation and total molecular number to shift from -1 power to -0.5 power. Owing to different chain reaction paths for high- and low-temperature auto-ignition, the strongest relative fluctuation occurs near the crossover temperature. A theoretical equation for the standard deviation of ignition delay time is obtained based on dimensional analysis, giving excellent agreement with the simulation results in both high- and low-temperature modes.

Published under an exclusive license by AIP Publishing. https://doi.org/10.1063/5.0154560

I. INTRODUCTION

The auto-ignition of a combustible mixture has been extensively studied over the past 70 years for its importance in combustion chemistry. Many studies considered the auto-ignition of a well-stirred mixture as a reaction kinetic process that is dictated by intensive quantities, such as temperature and density, but is immune to extensive quantities, such as volume. However, the reaction kinetic method, being a deterministic approach, cannot fully explain or predict random hotspots in low-temperature auto-ignition,[1,2] the scattered minimum ignition energy of a flame kernel,[3,4] and other fluctuations in microscale combustion. These phenomena are affected by various macroscopic disturbances and are also related to the microscopic fluctuations of molecular thermal motion. These microscopic fluctuations appear as volume decreases to the microscale and intensify in combustion through nonlinear

mechanisms such as thermal release and radical explosion. Various microscopic simulation methods have been considered to study the ignition problem, such as molecular dynamics (MD),[5] direct simulation Monte Carlo (DSMC),[6] and stochastic reaction kinetics.[7] Microscopic simulation results[8–11] indicate that the discrete and stochastic characteristics of reaction collisions cause significant fluctuations in the ignition process when the volume (or the total molecular number) is sufficiently small. However, the microscopic fluctuations in ignition are not fully understood due to the complexity of the reaction mechanism and limitations in simulation methods and computation capabilities.

The first research using MD[12] on the ignition problem appeared in 1984, which considered microscopic fluctuations in a thermal ignition system. Subsequent MD research[13,14] found that microscopic fluctuations are affected by the reaction model (especially the activation energy) and the total molecular number. In these

works, the reaction model is a simplified one-step reaction, and the total molecular number is only up to 10^4. Further improvements in the reaction model and simulation scale are challenging issues for MD. For the reaction model, each elemental reaction of an actual combustion system requires a corresponding potential energy surface, but currently, even for simple systems like the H_2–O_2 mixture, there is no complete database available. For the simulation scale, the computation cost of the MD method is high because the time step must be much smaller than the dynamic process of molecular collisions.

The DSMC method has also been used to simulate the thermal ignition problem.[8,15] The computation cost of the DSMC is much smaller than that of MD because the time step can be on the scale of the mean molecular collision time based on a decoupled treatment of the molecular motion and collisions. The decoupled treatment allows the DSMC to simulate an elemental reaction using phenomenological reaction models, whose parameters can be determined from the macroscopic reaction rates. The DSMC method was applied using phenomenological reaction models to simulate various combustion problems[16–18] for simple molecules such as H_2 and O_2. In our previous DSMC study of H_2–O_2 auto-ignition,[10] strong fluctuations in the ignition delay time were found when the total molecular number decreased from 10^7 to 10^5 at an initial temperature of 1500 K. However, the central processing unit (CPU) time required for DSMC simulations of auto-ignition increases significantly with an increase in the total molecular number or a decrease in the initial temperature. To obtain reliable statistical information on ignition delay time, a considerable number of independent DSMC realizations are necessary, rendering the computation exceedingly costly.

Besides molecular simulation methods, the master equation of a reacting system has also been used to study fluctuations in ignition.[8,19,20] In the field of stochastic reaction kinetics, this equation has a rigorous form called the chemical master equation (CME),[21] which describes the chemical reaction process similar to the reaction rate equation (RRE) but with a discrete and stochastic approach. Numerical methods have been developed to solve the CME, such as the stochastic simulation algorithm (SSA),[22] which is widely used to study biochemical problems in cellular systems.[23–25] Compared with molecular simulation methods, the computation cost of SSA is significantly reduced because the time step grows from the scale of molecular collisions to the scale of the chemical reaction. The SSA method is used to simulate CH_4-air auto-ignition using up to a few million molecules (corresponding to a volume of $(0.3\ \mu m)^3$,[9] and the distribution of the ignition delay time is obtained based on many realizations. The results indicate that the microscopic fluctuations in the ignition delay time increase for smaller initial temperatures and total molecular numbers, which agrees with our DSMC results of H_2–O_2 auto-ignition. However, the length scale of typical microscale combustion ranges from 1 μm to 1 mm, which is beyond the capability of SSA, especially when many realizations are needed for statistical averaging. As an approximate numerical procedure for the CME, the tau-leaping method[9] has a higher efficiency than the SSA when the system is sufficiently large. Previous studies[26,27] showed that the tau-leaping method may not perform well in a reaction system with rare species or reaction stiffness. Variations on the tau-leaping method are developed to improve simulation efficiency, such as the implicit tau-leaping

method,[28] the R-leaping method,[29] and the slow-scale tau-leaping method.[30] Additionally, hybrid simulations[31,32] of the tau-leaping method and its variants are proposed to further improve simulation efficiency and expand the range of applications.

This paper studies the microscopic behaviors of auto-ignition in a real combustion system through the stochastic reaction kinetic method. The H_2–O_2 mixture is considered representative due to its representative chain reaction mechanism. Section II illustrates the reaction kinetics of the H_2–O_2 mixture with a preliminary explanation of the microscopic auto-ignition. Section III develops a hybrid method of the SSA and tau-leaping methods for H_2–O_2 auto-ignition to provide greater efficiency than conventional methods. Section IV analyzes the stochastic simulation results of H_2–O_2 auto-ignition with a focus on the accumulation of stochasticity during ignition and the statistical characteristics of the final ignition delay time. The conclusions are given in Sec. V.

II. REACTION KINETICS

A well-established reaction mechanism[33] for H_2 and O_2 combustion is employed in this paper, consisting of 21 pairs of elemental reactions. Details of the reaction rates are found in the original paper. This section focuses on the chain reaction mechanism of radical production, which is critical to the ignition process at both the thermal dynamic limit (the total molecular number $N_{tot} \to \infty$) and the microscopic level.

A. Chain reaction mechanism

The H_2–O_2 auto-ignition consists of a relatively long stage of radical growth, called the induction period,[34] and a short heat-releasing stage marking the occurrence of ignition. A skeleton mechanism of eight elemental reactions[35] dominates the reaction process in the induction period, as shown in Table I. The reaction paths are shown in Fig. 1. Reaction No. 1 is the chain initiation reaction, which consumes fuel and oxidizer and generates the first radical H, initiating the subsequent chain propagation process. The subsequent chain propagation process, known as the three-step chain reaction, consists of reaction Nos. 2–4. In a complete three-step chain reaction, three H_2 and one O_2 are consumed, producing two H_2O and

TABLE I. Skeleton reaction mechanism of H_2–O_2 auto-ignition.

	Reaction	A^a	n^a	E^a
No. 1	$H_2 + O_2 \to H + HO_2$	2.04×10^{-17}	0.193	3.9×10^{-19}
No. 2	$H + O_2 \to OH + O$	5.85×10^{-14}	0.7	1.19×10^{-19}
No. 3	$O + H_2 \to OH + H$	8.4×10^{-26}	2.67	4.37×10^{-20}
No. 4	$H_2 + OH \to H_2O + H$	1.94×10^{-21}	1.3	2.52×10^{-20}
No. 5^b	$H + O_2 + M \to HO_2 + M$	1.59×10^{-40}	1.4	0
No. 6	$2HO_2 \to H_2O_2 + O_2$	5.01×10^{-18}	0	9.63×10^{-21}
No. 7	$HO_2 + H_2 \to H_2O_2 + H$	2.79×10^{-18}	0.336	1.73×10^{-19}
No. 8^c	$H_2O_2 + M \to 2OH + M$	4.85×10^{-7}	1.83	3.44×10^{-19}

^{a}Reaction-rate constant $k = AT^n e^{-E/RT}$. Units are molecule, s, m^{-3}, J and K.
^{b}Chaperon efficiencies are 2.5 for H_2, 12.0 for H_2O, and 1.0 for all other species.
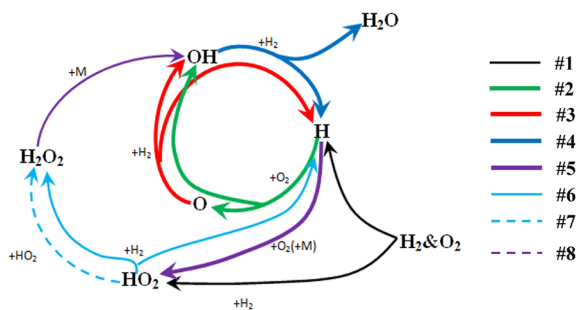^{c}Chaperon efficiencies are 2.0 for H_2, 6.0 for H_2O, and 1.0 for all other species.

FIG. 1. Reaction diagram of the skeleton mechanism.

FIG. 2. Ignition delay time calculated through the RRE.

two additional radical H. The additional radical H further accelerates the chain propagation process, leading to a radical explosion. At relatively low temperatures, the chain terminating reaction No. 5 competes with reaction No. 2 for H, significantly inhibiting the three-step chain reaction. Meanwhile, the HO_2 produced by reaction No. 5 leads to another chain propagation process through reaction Nos. 6–8, which play a crucial role in low-temperature auto-ignition. In this process, HO_2 converts to H_2O_2 through two exchange reaction (Nos. 6 and 7), followed by the conversion of H_2O_2 to OH through a dissociation reaction (No. 8). Finally, the generated OH reacts with H and H_2O through reaction No. 4.

The crossover temperature (called the extended second explosion limit, T_{2ed})[34] is often used to separate high- and low-temperature auto-ignitions. The crossover temperature is defined as

$$2k_{No.2}(T_{2ed}) = k_{No.5}(T_{2ed})n_{equi}, \tag{1}$$

in which $k_{No.i}$ is the reaction rate of reaction No. i and n_{equi} is an equivalent value of the molecular number density considering the third body coefficient. The default initial condition of the H_2–O_2 mixture is

$$n = 10^{25}\,\text{m}^{-3}, \quad \alpha_{H2} = 2/3, \quad \alpha_{O2} = 1/3,$$

where n is the number density and α is the mole fraction. The main parameters studied are the initial temperature T and the total molecular number N_{tot}. Using the default setting, T_{2ed} is 1016 K. In addition, it is assumed that the volume remains constant during the ignition process.

In the thermodynamic limit, the auto-ignition of a well-stirred mixture is described continuously and deterministically by the RRE. Figure 2 shows the ignition delay time calculated from the RRE using the CHEMKIN-II package.[36] The ignition delay time is when the temperature increases to 500 K above its initial value. In other literature, ignition delay time was also defined as the inflection point of a physical quantity (such as temperature, pressure, and radical concentration). However, this definition is not applicable to stochastic simulations due to the fluctuating nature of their time history, which leads to a derivative with pronounced noise. This noise poses a challenge in accurately locating the extremal point of the derivative, which corresponds to the inflection point. The ignition delay time ($t_{ig,RRE}$) increases for smaller initial temperatures. The temperature dependence of the ignition delay time changes greatly from
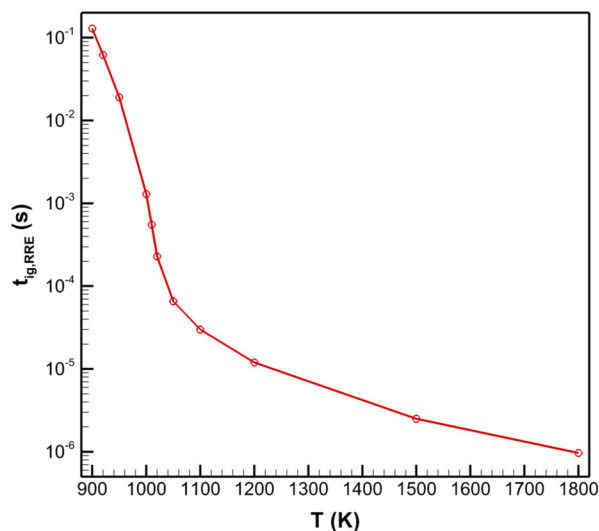
high to low temperatures because radical growth through reaction Nos. 6–8 is much slower than that through reaction Nos. 2–4.

Two typical auto-ignition processes are compared in Fig. 3 to explain the differences between the low- and high-temperature cases. The primary radicals in the induction period change from H/O/OH in the high-temperature case to HO_2/H_2O_2 in the low-temperature case. In both cases, H_2O is a vital reaction product and is used as a general symbol to mark the different auto-ignition stages.

B. Microscopic characteristics of auto-ignition

When N_{tot} is sufficiently small, auto-ignition is greatly influenced by the discrete and stochastic behaviors of each reaction collision, which are beyond the capability of continuous and deterministic approaches such as the RRE. A preliminary analysis explains how the microscopic characteristics of the reaction collision can influence auto-ignition when N_{tot} is sufficiently small. A full analysis is given in Sec. IV through the stochastic reaction kinetic method.

The first initiation reaction No. 1 is taken as an example. The firing time of reaction No. 1 obeys an exponential distribution, and its average and standard deviation are both equal to

$$t_{No.1} = (N_{tot} n k_{No.1} \alpha_{H2} \alpha_{O2})^{-1}. \tag{2}$$

Figure 4 presents a comparison between $t_{No.1}$ and $t_{ig,RRE}$, with a constant number density n. As N_{tot} decreases, $t_{No.1}$ increases and becomes comparable to and even larger than $t_{ig,RRE}$, indicating strong fluctuations in the ignition delay time and an increase in its average. To quantitatively analyze the influence of the initiation reaction, the critical value of N_{tot} is defined as when $t_{No.1}$ equals $t_{ig,RRE}$ as

$$N_{crit} = (t_{ig,RRE} n k_{No.1} \alpha_{H2} \alpha_{O2})^{-1}. \tag{3}$$

If N_{tot} is much larger than N_{crit}, the influence of $t_{No.1}$ can be neglected, and the actual ignition delay time converges to $t_{ig,RRE}$.

(a) T=1200 K

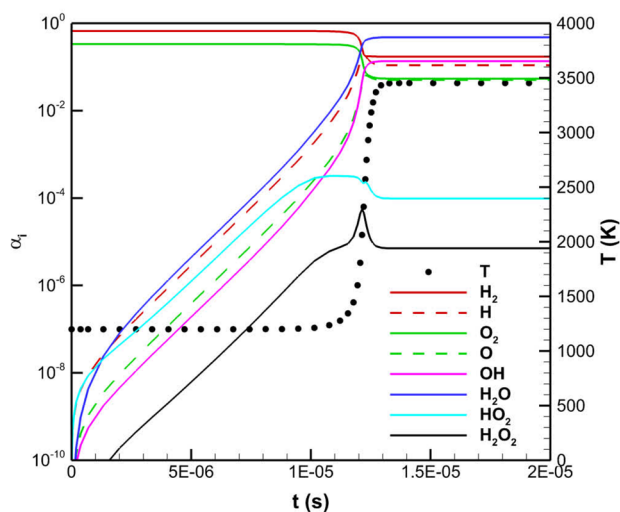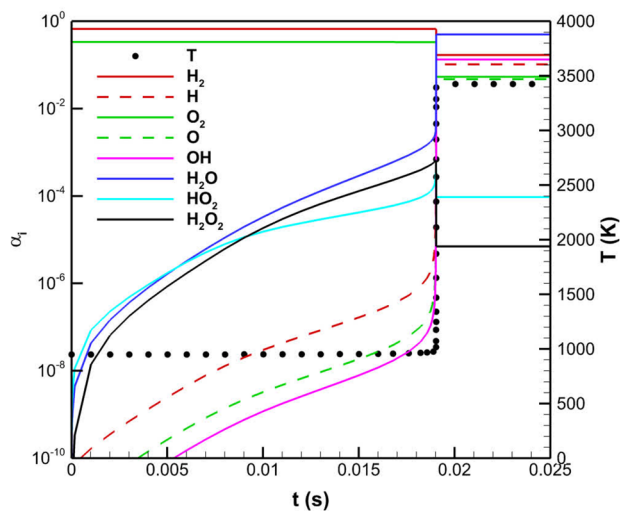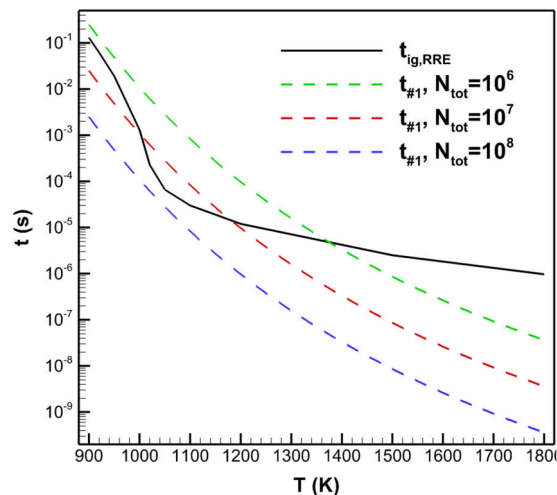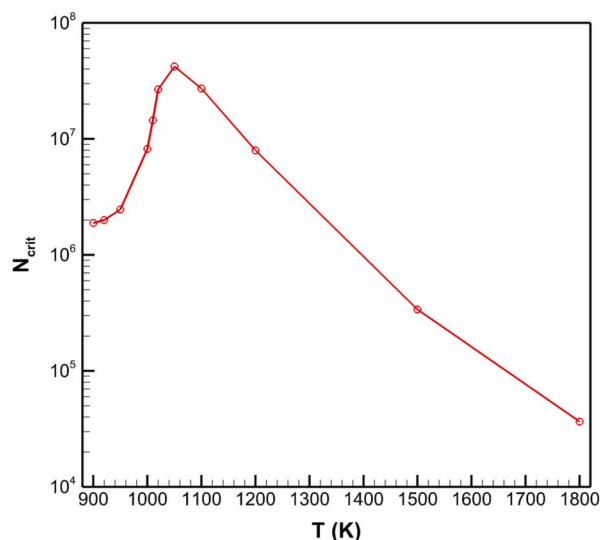FIG. 4. Comparison between $t_{No.1}$ and $t_{ig,RRE}$.

(b) T=950 K

FIG. 3. Auto-ignition processes as calculated through the RRE.

FIG. 5. The relationship between N_{crit} and T.

The relationship between N_{crit} and the initial temperature is shown in Fig. 5, and the maximum N_{crit} appears at 1050 K, indicating the stronger effect of $t_{No.1}$ near the crossover temperature.

III. HYBRID STOCHASTIC SIMULATION

The theoretical basis of stochastic reaction kinetics and two classical simulation methods are introduced. A hybrid approach is developed based on the classical methods, which brings greater efficiency for H_2–O_2 auto-ignition and other similar chain reaction systems.

A. Stochastic reaction kinetics

Consider a well-stirred system with N species and M reactions. The population of each species is X_i, and the state vector is $X = (X_1, \ldots, X_N)$. Each reaction No. j is characterized by two quantities: the propensity function a_j, which determines the probability that reaction No. j will occur in the next infinitesimal time interval, and the state change vector v_j, which determines the variations in X when reaction No. j occurs. The propensity function can be calculated using the reaction rate k. For example, initiation reaction No. 1 gives $a_{No.1} = Vn^2 k_{No.1} \alpha_{H2} \alpha_{O2}$.

In stochastic reaction kinetics, the fundamental equation is the CME as

$$\frac{\partial P(\boldsymbol{X}, t | \boldsymbol{X}_0, t_0)}{\partial t} = \sum_{j=1}^{M} \left[a_j(\boldsymbol{X} - \nu_j) P(\boldsymbol{X} - \nu_j, t | \boldsymbol{X}_0, t_0) - a_j(\boldsymbol{X}) P(\boldsymbol{X}, t | \boldsymbol{X}_0, t_0) \right], \tag{4}$$

where $P(\boldsymbol{X}, t | \boldsymbol{X}_0, t_0)$ is the probability that the state vector $\boldsymbol{X}_0$ at initial time t_0 becomes $\boldsymbol{X}$ at time t.

In the thermodynamic limit, Eq. (4) reduced to the RRE as

$$\frac{d\boldsymbol{X}}{dt} = \sum_{j=1}^{M} \left[\nu_j a_j(\boldsymbol{X}(t)) \right]. \tag{5}$$

As a coupled set of ordinary differential equations (ODEs), the CME can only be analytically solved for a few simple systems. Numerical approaches such as the SSA and tau-leaping methods are widely used to solve the CME for more complicated systems.

B. SSA method

The SSA method is a Monte Carlo procedure to numerically generate time trajectories of the molecular populations in accordance with the CME. For a state vector $\boldsymbol{X}(t)$, the following reaction time τ and reaction No. j are determined from a probability function as

$$p(\tau, j | \boldsymbol{X}, t) = a_j e^{-a_0 \tau}, \tag{6}$$

in which

$$a_0 = \sum_{j=1}^{M} a_j. \tag{7}$$

Based on Eq. (6), the numerical procedure used in this paper is given as follows:

(1) Calculate a_0 through Eq. (7).
(2) Generate a uniform random variable r_1 between 0 and one and calculate τ using the equation

$$\tau = \frac{1}{a_0} \ln\left(\frac{1}{r_1}\right). \tag{8}$$

(3) Generate a uniform random variable r_2 between 0 and one and determine j as the smallest integer satisfying the expression

$$\sum_{k=1}^{j} a_k > r_2 a_0. \tag{9}$$

(4) Update $\boldsymbol{X}$ and t using ν_j and τ.

C. Tau-leaping method

The SSA method simulates one reaction event at a time, making it relatively slow when dealing with a large number of reaction events. Alternatively, the tau-leaping method advances the system through many reaction events in a single time step. Assuming the propensity function of reaction No. j does not change significantly over a small time step τ, the number of times this reaction fires can be approximated by a Poisson random variable P_j with a mean value of $a_j\tau$. Therefore, the tau-leaping method generates a possible time trajectory of $\boldsymbol{X}(t)$ as

$$\boldsymbol{X}(t + \tau) = \boldsymbol{X}(t) + \sum_{j=1}^{M} \left[P_j(a_j\tau)\nu_j \right]. \tag{10}$$

As a core issue in the tau-leaping method, the time step restriction (also called the leaping condition) can be determined indirectly.[37] The basic idea is to bound $\Delta x_i/x_i$ rather than $\Delta a_j/a_j$ by a small value ε_i. Here, $\varepsilon_i = 0.001$.

The numerical procedure is given as follows:

(1) Calculate the time step τ satisfying the leaping condition.
(2) For each reaction No. j, generate a Poisson random variable P_j with a mean equal to $a_j\tau$.
(3) Update $\boldsymbol{X}$ and t through Eq. (10).

D. Hybrid SSA and tau-leaping method

The tau-leaping method is more efficient than the SSA when the $a_j\tau$ of each reaction is much larger than one, which is generally satisfied for large systems. However, if the reaction process involves rare species that may restrict the time step to a small value, the efficiency of tau-leaping decreases dramatically. This problem exists in H_2–O_2 auto-ignition because the number of radicals is relatively small in the early stage. The problem becomes even more significant in low-temperature auto-ignition because H/O/OH remain at very low concentrations over nearly the entire induction period [see Fig. 3(b)].

This problem is alleviated through the proposed hybrid SSA and tau-leaping methods. In the early stages of the induction period, the SSA method has good efficiency. It ensures accurate predictions of key stochastic characteristics, such as fluctuations the initiation reaction. Due to the radical explosion in the induction period, the total reaction rate grows, and the tau-leaping method becomes more efficient. The fundamental procedure of the hybrid method is selecting an appropriate point to switch from the SSA to tau-leaping to optimize the simulation efficiency. The switch point is defined as the state when a specific variable reaches a critical value. The population of a particular species is more appropriate than the temperature because the latter does not change much during the induction period. Therefore, the population of H_2O is chosen to define different states of the induction period due to its applicability in both high- and low-temperature cases.

Figure 6 shows the average CPU time costs of the hybrid method with various switch points for a specific case. For this case, the appropriate switch point is ~50 000. However, this requires testing many switch points, and each switch point includes several realizations to obtain the average CPU time cost. Here we provide a more convenient procedure to determine the appropriate switch point, which requires only two specific realizations. For a particular case, the procedure is given as follows:

(1) Simulate realizations using the SSA and tau-leaping. Record the CPU time cost when N_{H2O} reaches different values, i.e., $t_{SSA}(N_{H2O})$ and $t_{tau-leaping}(N_{H2O})$.
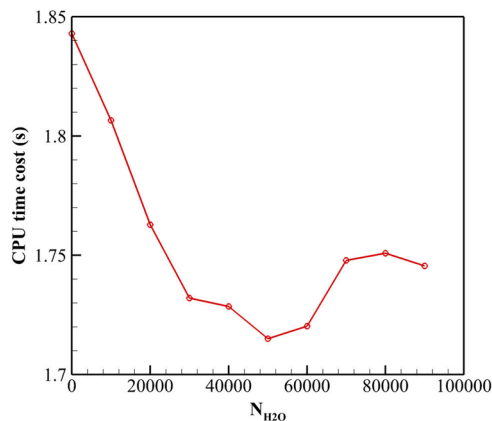
FIG. 6. Average CPU time cost of the hybrid method with different switch points. The simulation is terminated at the moment of ignition at $T = 1200$ K and $N_{tot} = 10^{10}$.
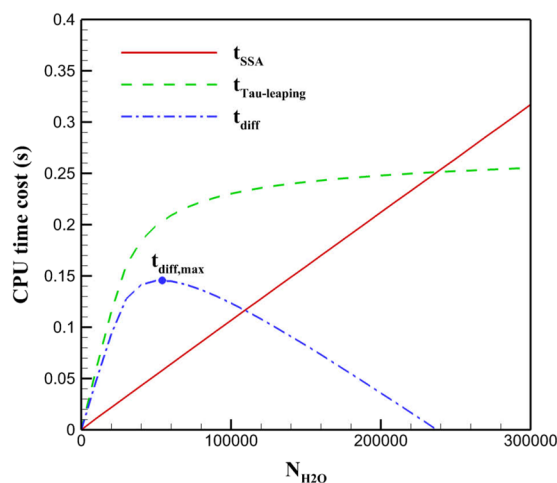
(2) Calculate the difference between t_{SSA} and $t_{tau-leaping}$ as
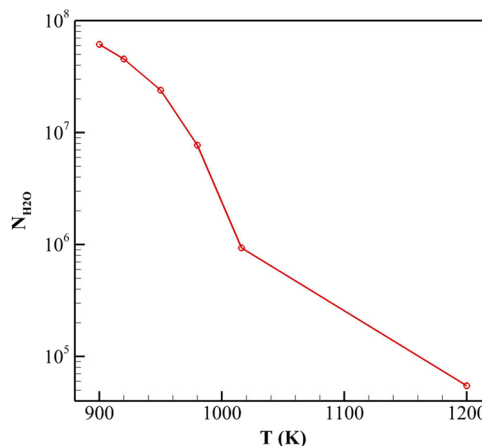
$$t_{diff}(N_{H_2O}) = t_{tau-leaping}(N_{H_2O}) - t_{SSA}(N_{H_2O}). \quad (11)$$

(3) Find the maximum value of $t_{diff}(N_{H_2O})$, and use the corresponding N_{H_2O} as the appropriate switch point.

Figure 7 gives the results for the t_{SSA}, $t_{tau-leaping}$, and t_{diff} under the same case shown in Fig. 6. The maximum of t_{diff} corresponds to $N_{H_2O} = 54\,000$, which agrees with Fig. 6. It should be noted that the hybrid method is applicable to more generalized systems. Depending on the specific problem, multiple switch points may exist, and they can be conveniently identified using the procedures given earlier.

The appropriate switch point was determined between 900 and 1200 K using the above-mentioned procedure, as shown in Fig. 8. The average CPU time cost is compared between the hybrid method


FIG. 8. The appropriate switch point of the hybrid method for auto-ignition between 900 and 1200 K with $N_{tot} = 10^{10}$.

using the appropriate switch and the tau-leaping method, as shown in Fig. 9. Although the average CPU time cost for both methods increases with smaller temperatures, the growth of the hybrid method is slower than that of the tau-leaping method. Therefore, relative reductions in the CPU time cost ($1 - t_{hybrid}/t_{tau-leaping}$) increase for smaller temperatures, as shown in Fig. 10. The relative reduction is over 70% at 900 K, resulting in an absolute reduction ($t_{tau-leaping} - t_{hybrid}$) of over 4 min. This significant improvement in simulation efficiency is particularly advantageous when conducting statistical averaging with multiple realizations at low temperatures. In addition, when numerically solving a chemically reacting fluid problem using the stochastic reaction–diffusion equation, the computational cost of reaction kinetics can be much larger than that of molecular diffusion, especially for complex reaction mechanisms. Therefore, the hybrid method can significantly reduce the overall computational cost. The appropriate switch points above 1200 K are not given because the two methods have little difference in simulation efficiency at relatively high temperatures.

FIG. 7. Comparison between t_1 and $t_{ig,RRE}$.
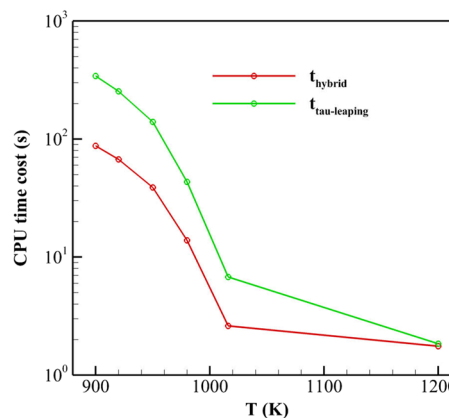
FIG. 9. Comparison of the CPU time costs for hybrid and tau-leaping methods for auto-ignition from 900 to 1200 K with $N_{tot} = 10^{10}$.

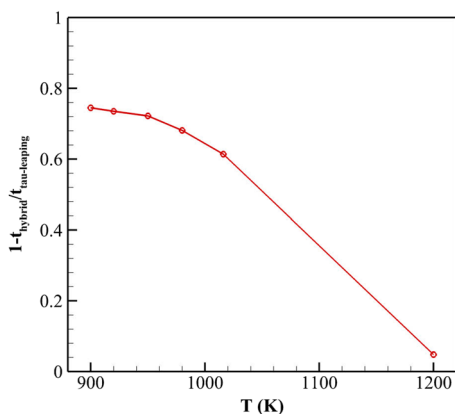**FIG. 10.** Relative reduction in the CPU time cost ($1 - t_{hybrid}/t_{tau-leaping}$) for auto-ignition from 900 to 1200 K with $N_{tot} = 10^{10}$.

It should be noted that the CPU time cost of the hybrid method is still quite large at 900 K. The reason is that the appropriate switch point becomes very large in low temperature auto-ignition due to the existence of rare species (H/O/OH) in almost the whole induction period [see Fig. 3(b)]. Stochastic reaction systems with similar problems are referred to as stochastic stiffness systems. An effective way to solve this problem is to separate the stiff system into a slow subset and a fast subset. The slow subset is simulated by the SSA method or the tau-leaping method. The fast subset, which has little impact on the entire system, is determined by its stationary state, as in the slow-scale SSA method[38] and the slow-scale tau-leaping method,[30] or simulated by the RRE, as in the HR method.[39] These methods require the time scale for the fast subset to relax to its stationary state to be much shorter than the time scale for reactions
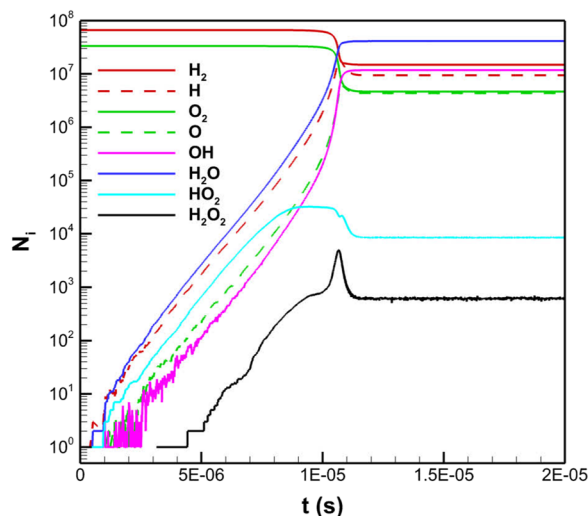
in the slow subset to occur. However, this is not satisfied in H_2–O_2 auto-ignition and is not used in the present study.

IV. ANALYSIS OF SIMULATION RESULTS

The simulation results under different initial conditions (i.e., T and N_{tot}) are obtained using the hybrid method. Typical realizations are shown first, and the statistical properties are analyzed for the ignition process and ignition delay time.
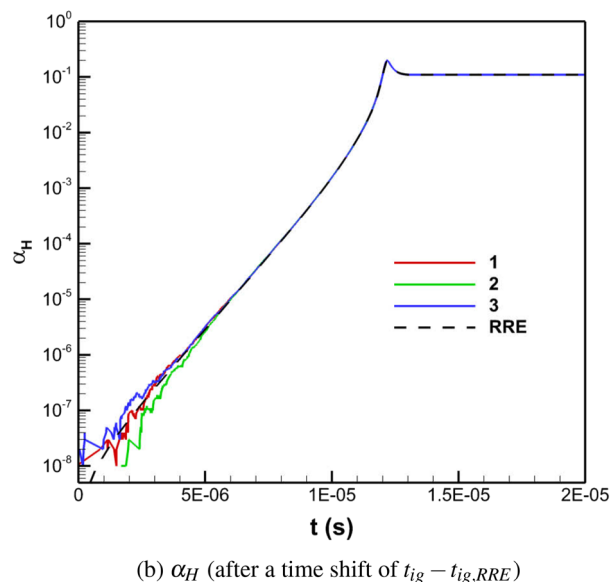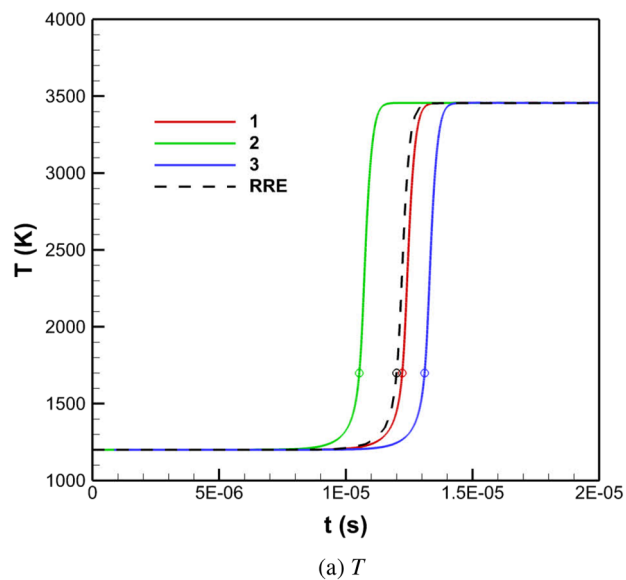

(a) T

(b) α_H (after a time shift of $t_{ig} - t_{ig,RRE}$)

FIG. 12. Comparison of three possible realizations with $T = 1200$ K and $N_{tot} = 10^8$. The curves 1, 2, and 3 correspond to ignition close to, before, and after the RRE results.

FIG. 11. Time history of the species population for auto-ignition with $T = 1200$ K and $N_{tot} = 10^8$.

A. Typical realizations

One realization of H_2–O_2 auto-ignition is shown in Fig. 11. The initial condition is $T = 1200$ K and $N_{tot} = 10^8$. In the early stages, the time histories of the radicals show strong fluctuations, indicating the chain reactions are highly stochastic when the radical population is small. As the radical population increases, the time histories show a deterministic characteristic similar to the RRE results. However, the accumulated stochasticity of the early stage is preserved in the ignition process, which influences the ignition delay time.

Figure 12 compares three possible realizations: ignition close to, before, and after the RRE results. Figure 12(a) compares the time history of the temperature, and the ignition delay time (t_{ig}) for each realization is marked in the curve. Figure 12(b) compares the time histories of the mole fraction of H after a time shift of $t_{ig} - t_{ig,RRE}$. Differences between each curve only exist when α_H is smaller than 10^{-5}, confirming that fluctuations in auto-ignition come primarily from the early induction period.

B. Statistical analysis of the ignition process

The statistical properties of different states for auto-ignition are analyzed to explain the accumulation of stochasticity during ignition. Similar to Sec. III D, the H_2O population defines a specific auto-ignition state, and the statistical properties when N_{H2O} reaches a specific value are obtained by averaging 10^4 realizations for each condition. Figure 13 shows the standard deviation of the physical time to reach different states, representing accumulated stochasticity in the induction period. The standard deviation increases rapidly in the early stage and then remains almost constant after $N_{H2O} > 1000$, corresponding to a mole fraction of 10^{-5}.

Figure 14 shows the probability distributions of $N_H - N_{H,avg}$ and $(N_H - N_{H,avg})/N_{H,avg}$ at different states, which represent the absolute and relative fluctuations of N_H. As the ignition process advances, the absolute fluctuations increase while the relative fluctuations decrease. Due to the decreased relative fluctuations,
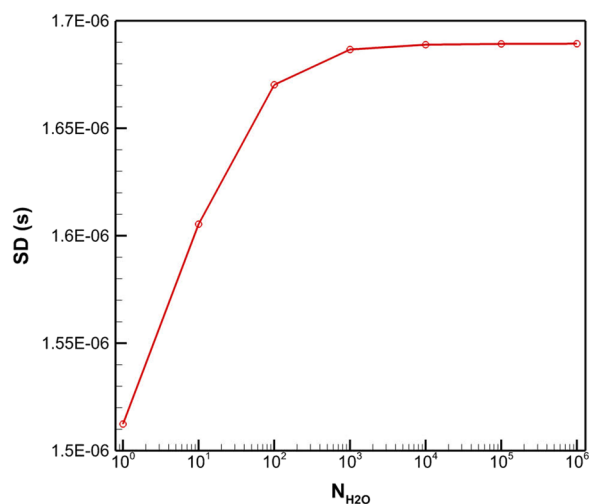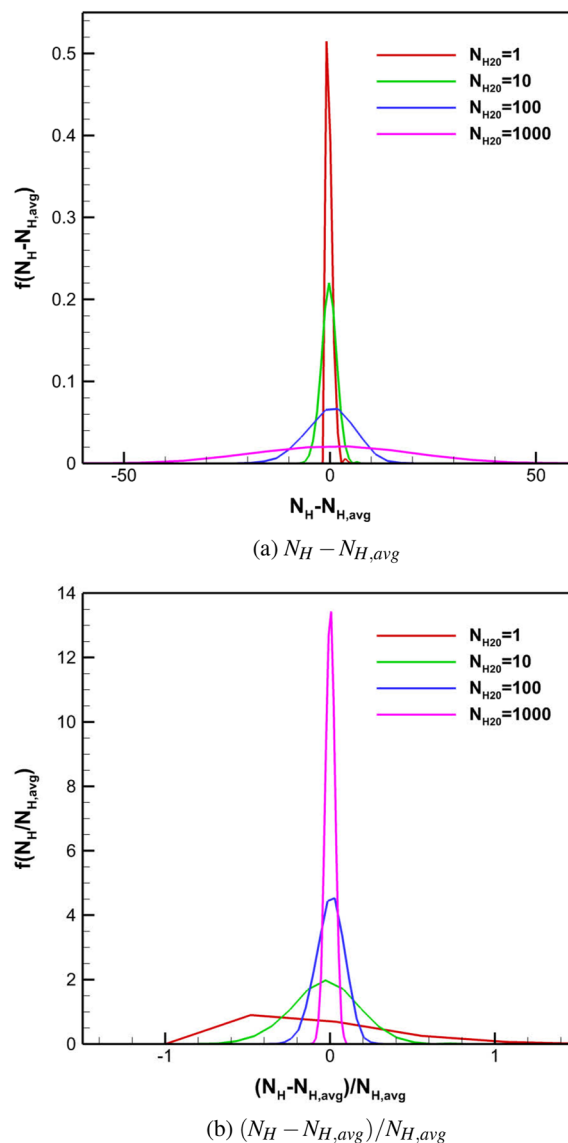

(a) $N_H - N_{H,avg}$

(b) $(N_H - N_{H,avg})/N_{H,avg}$

FIG. 14. Probability distribution of N_H at different states with $T = 1200$ K and $N_{tot} = 10^8$.

chain reactions that take radicals as reactants tend to be more deterministic. Similar results are found for O and OH.

C. Statistical analysis of ignition delay time

The accumulated stochasticity causes the ignition delay time to fluctuate around its average value. The statistical properties of the ignition delay time are closely related to the initial conditions, such as N_{tot} and T, which are analyzed here.

1. Influence of N_{tot}

The probability distribution of the ignition delay time $f(t_{ig})$ is given first as a straightforward explanation for the fluctuations in
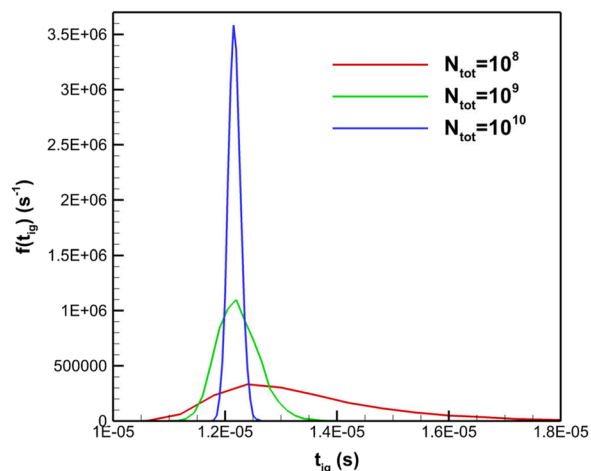

FIG. 13. Standard deviation (SD) of the physical time to reach different states with $T = 1200$ K and $N_{tot} = 10^8$.

FIG. 15. Probability distribution of t_{ig} for different N_{tot} with T = 1200 K.

FIG. 17. Relationship between the standard deviation of the ignition delay time and N_{tot} with T = 1200 K. The powers of the fit lines are −0.957 (green) and −0.499 (blue).

the ignition delay time. Figure 15 compares $f(t_{ig})$ for different N_{tot} with an initial temperature of 1200 K. As N_{tot} decreases, fluctuations in the ignition delay time increase. Meanwhile, the average ignition delay time has a noticeable increase as N_{tot} decreases to 10^8.

Figure 16 shows the relationship between the average ignition delay time $t_{ig,avg}$ and N_{tot} with an initial temperature of 1200 K. When N_{tot} is sufficiently large, $t_{ig,avg}$ becomes identical to $t_{ig,RRE}$. When N_{tot} is sufficiently small, $t_{ig,avg}$ approaches the average time of the initiation reaction $t_{No.1}$. For $N_{tot} = 10^8$, $t_{ig,avg}$ is 10.8% larger than $t_{ig,RRE}$. This result can also be inferred from Fig. 4, which shows that $t_{No.1}$ is comparable to $t_{ig,RRE}$ for T = 1200 K and $N_{tot} = 10^8$ (about one order of magnitude smaller).

Figure 17 shows the relationship between the standard deviation of the ignition delay time SD_{ig} and N_{tot} with an initial
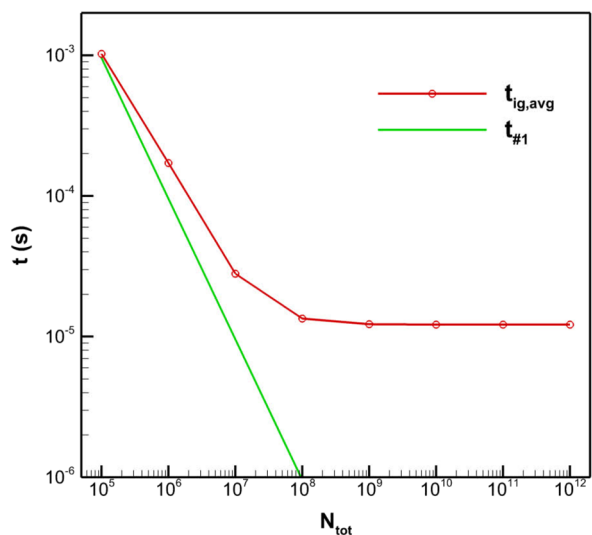
temperature of 1200 K. Two different power laws well describe the relationship. The power is ∼−1 when N_{tot} is sufficiently small and ∼−0.5 when N_{tot} is sufficiently large. Similar results were also found at temperatures below the crossover temperature, as shown in Fig. 18. The −1 power is from fluctuations in the initiation reaction [see Eq. (2)], while the −0.5 power is from both the initiation reaction and the following chain reactions. The latter relation is common for a sufficiently large system, which can be explained through the

FIG. 16. Average ignition delay time for different N_{tot} with T = 1200 K.
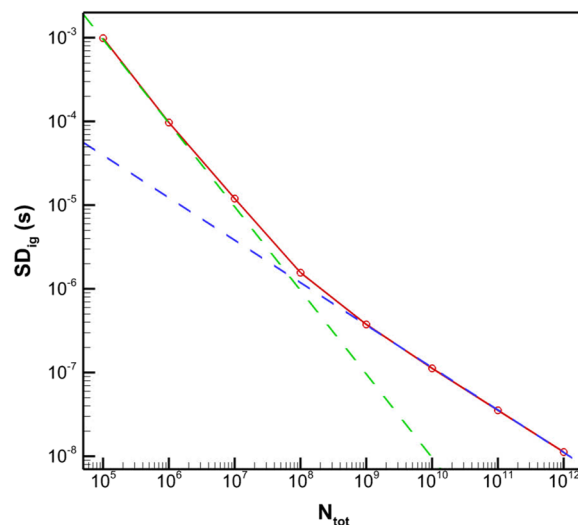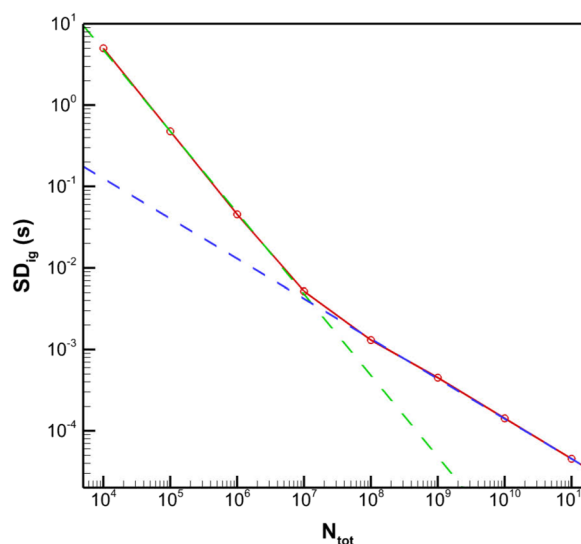

FIG. 18. Relationship between the standard deviation of the ignition delay time and N_{tot} with T = 950 K. The powers of the fit lines are −0.998 (green) and −0.492 (blue).
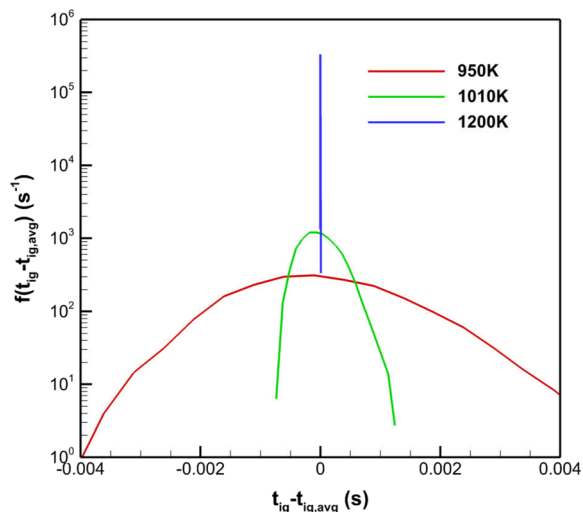
FIG. 19. Probability distribution of $t_{ig} - t_{ig,avg}$ for different initial temperatures with $N_{tot} = 10^8$.

chemical Langevin equation (CLE)[40] (an approximation of the CME for sufficiently large systems).

2. Influence of T

The probability distribution of $t_{ig} - t_{ig,avg}$ represents the absolute fluctuations of the ignition delay time and is compared in Fig. 19 with different initial temperatures and a N_{tot} of 10^8. The significant increase in ignition delay time when the initial temperature decreases causes the absolute fluctuations to grow significantly and require a logarithmic coordinate system for the vertical
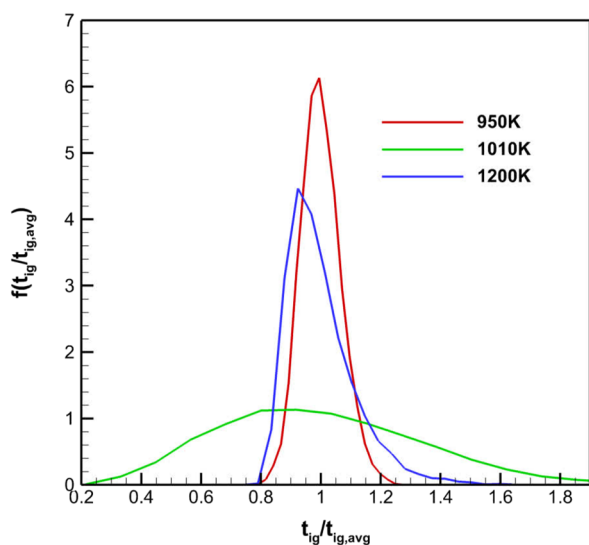

FIG. 20. Probability distribution of $t_{ig}/t_{ig,avg}$ for different initial temperatures with $N_{tot} = 10^8$.
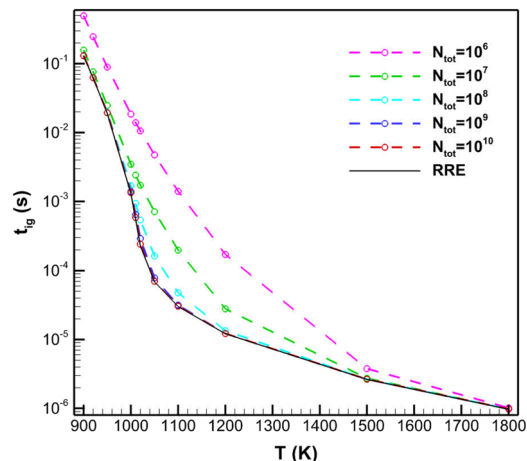

FIG. 21. Relationship between $t_{ig,avg}$ and the initial temperature with $N_{tot} = 10^6$–10^{10}.

axis. The probability distribution of $t_{ig}/t_{ig,avg}$ represents the relative fluctuations in the ignition delay time and is compared in Fig. 20. The relative fluctuations for 1010 K are much larger than those for 950 and 1200 K, indicating that the intensity of the relative fluctuations changes non-monotonically near the crossover temperature.

Figure 21 illustrates the relationship between $t_{ig,avg}$ and the initial temperature for several fixed N_{tot}. Although $t_{ig,avg}$ for all temperatures approaches $t_{ig,RRE}$ as N_{tot} increases, the convergence speed is slower near the crossover temperature due to the greater influence of $t_{No.1}$, which agrees with the results in Fig. 5.

The relationship between SD_{ig} and the initial temperature is plotted in Fig. 22 for two different values of N_{tot}. For N_{tot} of 10^6, which is in the −1 power-law regime, fluctuations are determined by the initiation reaction; therefore, SD_{ig} is in good agreement with
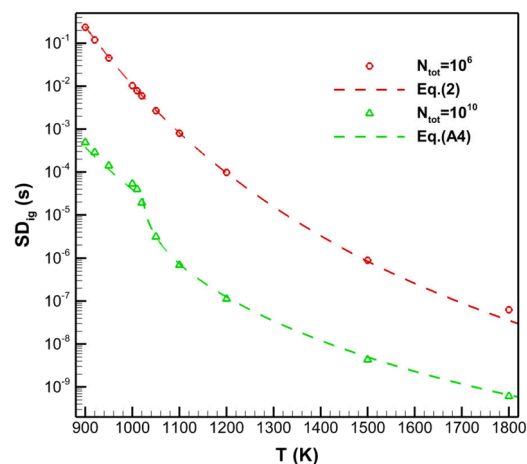

FIG. 22. Relationship between the SD_{ig} and the initial temperature with $N_{tot} = 10^6$ and 10^{10}.
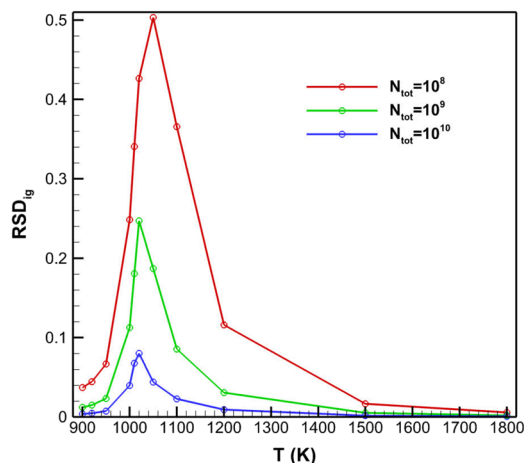
FIG. 23. The relative standard deviation of the ignition delay time.

$t_{No.1}$ [see Eq. (2)]. For N_{tot} of 10^{10}, which is in the -0.5 power-law regime, fluctuations are determined by the initiation reaction and the subsequent chain reactions. A theoretical equation for SD_{ig} is obtained for the -0.5 power-law regime using dimensional analysis. A detailed derivation is in the Appendix, and Eq. (A4) is the final result. By setting $C_1 = C_2 = 1$ [parameters in Eq. (A4)], excellent agreement is achieved between the theoretical equation and the stochastic simulation results, as shown in Fig. 22.

The relative standard deviation of the ignition delay time (RSD_{ig}) is defined as the standard deviation of $t_{ig}/t_{ig,avg}$, as shown in Fig. 23. The RSD_{ig} changes non-monotonically with temperature, and the maximum RSD_{ig} appears near the crossover temperature, which confirms the results from Fig. 19. For N_{tot} of 10^{10}, which corresponds to a volume of $(10\ \mu m)^3$, the RSD_{ig} at 1020 K is 8%. The scale of 10 μm coincides with some physical scales of microscale combustion, such as the Kolmogorov scale in turbulent combustion, which is usually on the order of 10–100 μm. Therefore, the microscopic characteristics of auto-ignition may affect microscale combustion at the crossover temperature and other extreme conditions. Similar topics have been discussed in the literature as well. The impact of thermal fluctuations on non-reactive turbulence was studied through fluctuating hydrodynamics,[41,42] revealing that these fluctuations dominate the energy spectrum at length scales comparable to the Kolmogorov length. For turbulent combustion, scalar fluctuation and its dissipation rate were widely studied[43,44] in the fluid dynamics community, but the influence of thermal fluctuations was omitted in relevant papers. To investigate thermal fluctuations in chemically reacting flows, future studies could consider employing fluctuating hydrodynamics and stochastic chemistry.

V. CONCLUSION

A hybrid stochastic simulation method is developed to simulate H_2–O_2 auto-ignition at the microscale. Typical realizations and statistical properties are analyzed to fully study the microscopic characteristics of the ignition process and ignition delay time. The main conclusions are given as follows.

When N_{tot} is sufficiently large, the ignition process calculated from the stochastic simulations is identical to the calculations from the RRE. As N_{tot} decreases, strong fluctuations appear in the time history of the radical populations, leading to stochastic behavior in the ignition process. The stochasticity that accumulates in the ignition process grows rapidly in the early stages but stabilizes in the later stages as the relative fluctuations in the radical population decrease.

Due to the accumulated stochasticity, the ignition delay time fluctuates around its average. The SD_{ig} grows for the smaller N_{tot}, and two power laws well describe the relationship between SD_{ig} and N_{tot}. The power law is close to -1 when N_{tot} is sufficiently small and is close to -0.5 when N_{tot} is sufficiently large. A theoretical equation for SD_{ig} is obtained using the power law relationship and dimensional analysis, which agrees well with the simulation results.

As N_{tot} decreases to the order of 10^8, there is an increase in $t_{ig,avg}$. This is primarily because the firing time of the first initiation reaction grows and becomes comparable to the ignition delay time. Due to the different chain reaction mechanisms involved in high- and low-temperature auto-ignition, the increase in $t_{ig,avg}$ is more pronounced near the crossover temperature. The RSD_{ig} also reaches its maximum near the crossover temperature.

The diffusion-reaction master equation may be used in future research to explore the microscopic characteristics of molecular diffusion in combustion phenomena.

AUTHOR DECLARATIONS

Conflict of Interest

The authors have no conflicts to disclose.

Author Contributions

C. Yang: Conceptualization (equal); Data curation (lead); Formal analysis (lead); Funding acquisition (equal); Investigation (lead); Methodology (lead); Project administration (lead); Resources (lead); Software (lead); Validation (lead); Visualization (lead); Writing – original draft (lead); Writing – review & editing (lead). **Y. Hu**: Writing – review & editing (supporting). **X. Y. Wang**: Visualization (supporting). **Q. Z. Hong**: Resources (supporting). **Q. H. Sun**: Conceptualization (equal); Formal analysis (supporting); Funding acquisition (equal); Investigation (supporting); Methodology (supporting); Project administration (supporting); Resources (supporting); Software (supporting); Supervision (lead); Writing – review & editing (supporting).

DATA AVAILABILITY

The data that support the findings of this study are available within the article.

APPENDIX: APPENDIXES

When $T > T_{2ed}$, the reaction process is determined primarily by the initiation reaction (No. 1) and the three-step chain reaction (Nos. 2–4). Radical production through the three-step chain reaction is determined primarily by the rate of reaction No. 2 when the mixture is neither too lean nor too rich. Therefore, the equation should consider four key parameters (N_{tot}, n, $k_1\alpha_{H2}\alpha_{O2}$, $k_2\alpha_{O2}$), which consist of three dimensions (mass, length, and time). According to the Pi theorem, we derive the relationship between two nondimensional parameters as

$$\sigma_{ig} n k_{No.2}\alpha_{O2} = f\left(\frac{N_{tot} \cdot k_{No.1}\alpha_{H2}\alpha_{O2}}{k_{No.2}\alpha_{O2}}\right). \tag{A1}$$

Using the conclusion that the SD_{ig} is proportional to $N_{tot}^{0.5}$ when N_{tot} is relatively large, Eq. (A1) can be converted to

$$\sigma_{ig} = C_1\left(N_{tot} \cdot n^2 \cdot k_{No.1}\alpha_{H2}\alpha_{O2} \cdot k_{No.2}\alpha_{O2}\right)^{-0.5}. \tag{A2}$$

Similarly, when $T < T_{2ed}$, Eq. (A1) can be converted to

$$\sigma_{ig} = C_2\left(N_{tot} \cdot n^2 \cdot k_{No.1}\alpha_{H2}\alpha_{O2} \cdot k_{No.7}\alpha_{H2}\right)^{-0.5}. \tag{A3}$$

The influence of chain terminating reaction No. 5 is introduced into Eq. (A2) to improve the accuracy near the crossover temperature. This reflects the modifications of $k_{No.1}$ and $k_{No.2}$. The modified expression is

$$\sigma_{ig} = C_1\left(N_{tot} \cdot n^2 \cdot k_{No.1}\left(1 - \frac{k_{No.5}n_M}{2k_{No.2}}\right)\right.$$
$$\left. \times \alpha_{H2}\alpha_{O2} \cdot (k_{No.2} - 0.5k_{No.5}n_M)\alpha_{O2}\right)^{-0.5}, \tag{A4a}$$

$$\sigma_{ig} = C_2\left(N_{tot} \cdot n^2 \cdot k_{No.1}\alpha_{H2}\alpha_{O2} \cdot k_{No.7}\alpha_{H2}\right)^{-0.5}. \tag{A4b}$$

In practice, the transition point between the high- and low-temperature expressions is set to be 5 K greater than T_{2ed}. Therein, the singularity is avoided when $T = T_{2ed}$ is avoided, and the SD_{ig} near the crossover temperature can be approximated.

REFERENCES

[1] R. Blumenthal, K. Fieweger, K. Komp, and G. Adomeit, "Gas dynamic features of self ignition of non diluted fuel/air mixtures at high pressure," Combust. Sci. Technol. **113**, 137–166 (1996).

[2] M. Drake and D. Haworth, "Advanced gasoline engine development using optical diagnostics and numerical modeling," Proc. Combust. Inst. **31**, 99–124 (2007).

[3] Z. Chen, M. P. Burke, and Y. Ju, "On the critical flame radius and minimum ignition energy for spherical flame initiation," Proc. Combust. Inst. **33**, 1219–1226 (2011).

[4] A. Wähner, G. Gramse, T. Langer, and M. Beyer, "Determination of the minimum ignition energy on the basis of a statistical approach," J. Loss Prev. Process Ind. **26**, 1655–1660 (2013).

[5] M. P. Allen and D. J. Tildesley, *Computer Simulation of Liquids* (Oxford University Press, 2017).

[6] G. A. Bird, *Molecular Gas Dynamics and the Direct Simulation of Gas Flows* (Clarendon Press, 1994).

[7] D. T. Gillespie, "Stochastic simulation of chemical kinetics," Annu. Rev. Phys. Chem. **58**, 35–55 (2007).

[8] B. Nowakowski and A. Lemarchand, "Thermal explosion near bifurcation: Stochastic features of ignition," Physica A **311**, 80–96 (2002).

[9] A. Frisque, J. Schnakenberg, J. Huang, and W. Bushe, "Stochastic simulation of variations in the autoignition delay time of premixed methane and air," Combust. Theory Modell. **10**, 241–256 (2006).

[10] C. Yang and Q. Sun, "Investigation of spontaneous combustion of hydrogen-oxygen mixture using DSMC simulation," AIP Conf. Proc. **1628**, 1261–1267 (2014).

[11] N. Sirmas and M. I. Radulescu, "Thermal ignition revisited with two-dimensional molecular dynamics: Role of fluctuations in activated collisions," Combust. Flame **177**, 79–88 (2017).

[12] D.-P. Chou and S. Yip, "Molecular dynamics simulation of thermal ignition in a reacting hard sphere fluid," Combust. Flame **58**, 239–253 (1984).

[13] J. Gorecki and J. Gryko, "The adiabatic thermal explosion in a small system: Comparison of the stochastic approach with the molecular dynamics simulation," J. Stat. Phys. **48**, 329–342 (1987).

[14] J. Gorecki and J. N. Gorecka, "Molecular dynamics simulations of nonequilibrium rate constant in a model exothermic reaction," Chem. Phys. Lett. **319**, 173–178 (2000).

[15] B. Nowakowski and A. Lemarchand, "Sensitivity of explosion to departure from partial equilibrium," Phys. Rev. E **68**, 031105 (2003).

[16] G. Bird, "Chemical reactions in DSMC," AIP Conf. Proc. **1333**, 1195–1202 (2011).

[17] Y. A. Bondar, K. Maruta, and M. S. Ivanov, "Hydrogen-oxygen detonation study by the DSMC method," AIP Conf. Proc. **1333**, 1209–1214 (2011).

[18] I. B. Sebastião, L. Qiao, and A. Alexeenko, "Direct simulation Monte Carlo modeling of H₂–O₂ deflagration waves," Combust. Flame **198**, 40–53 (2018).

[19] F. Baras, G. Nicolis, M. M. Mansour, and J. Turner, "Stochastic theory of adiabatic explosion," J. Stat. Phys. **32**, 1–23 (1983).

[20] B. Nowakowski and A. Lemarchand, "Stochastic effects in a thermochemical system with Newtonian heat exchange," Phys. Rev. E **64**, 061108 (2001).

[21] D. T. Gillespie, "A rigorous derivation of the chemical master equation," Physica A **188**, 404–425 (1992).

[22] D. T. Gillespie, "A general method for numerically simulating the stochastic time evolution of coupled chemical reactions," J. Comput. Phys. **22**, 403–434 (1976).

[23] H. H. McAdams and A. Arkin, "Stochastic mechanisms in gene expression," Proc. Natl. Acad. Sci. U. S. A. **94**, 814–819 (1997).

[24] L. S. Weinberger, J. C. Burnett, J. E. Toettcher, A. P. Arkin, and D. V. Schaffer, "Stochastic gene expression in a lentiviral positive-feedback loop: HIV-1 Tat fluctuations drive phenotypic diversity," Cell **122**, 169–182 (2005).

[25] A. K. Lam and R. Dutzler, "Mechanism of pore opening in the calcium-activated chloride channel TMEM16A," Nat. Commun. **12**, 786 (2021).

[26] M. Rathinam, L. R. Petzold, Y. Cao, and D. T. Gillespie, "Stiffness in stochastic chemically reacting systems: The implicit tau-leaping method," J. Chem. Phys. **119**, 12784–12794 (2003).

[27] J. Fu, S. Wu, and L. R. Petzold, "Time dependent solution for acceleration of tau-leaping," J. Comput. Phys. **235**, 446–457 (2013).

[28] M. Rathinam, L. R. Petzold, Y. Cao, and D. T. Gillespie, "Consistency and stability of tau-leaping schemes for chemical reaction systems," Multiscale Model. Simul. **4**, 867–895 (2005).

[29] A. Auger, P. Chatelain, and P. Koumoutsakos, "R-leaping: Accelerating the stochastic simulation algorithm by reaction leaps," J. Chem. Phys. **125**, 084103 (2006).

[30] Y. Cao and L. Petzold, "Slow-scale tau-leaping method," Comput. Methods Appl. Mech. Eng. **197**, 3472–3479 (2008).

[31] Y. Cao, D. T. Gillespie, and L. R. Petzold, "Adaptive explicit-implicit tau-leaping method with automatic tau selection," J. Chem. Phys. **126**, 224101 (2007).

[32] J. Lipková, G. Arampatzis, P. Chatelain, B. Menze, and P. Koumoutsakos, "S-leaping: An adaptive, accelerated stochastic simulation algorithm, bridging τ-leaping and r-leaping," Bull. Math. Biol. **81**, 3074–3096 (2019).

[33] P. Saxena and F. A. Williams, "Testing a small detailed chemical-kinetic mechanism for the combustion of hydrogen and carbon monoxide," Combust. Flame **145**, 316–323 (2006).

[34] G. D. Álamo, F. A. Williams, and A. L. Sánchez, "Hydrogen–oxygen induction times above crossover temperatures," Combust. Sci. Technol. **176**, 1599–1626 (2004).

[35] P. Boivin, A. L. Sánchez, and F. A. Williams, "Explicit analytic prediction for hydrogen–oxygen ignition times at temperatures below crossover," Combust. Flame **159**, 748–752 (2012).

[36] R. J. Kee, F. M. Rupley, and J. A. Miller, "Chemkin-II: A fortran chemical kinetics package for the analysis of gas-phase chemical kinetics," Technical Report No. SAND-89-8009, Sandia National Laboratories(SNL-CA), Livermore, CA, 1989.

[37] Y. Cao, D. T. Gillespie, and L. R. Petzold, "Efficient step size selection for the tau-leaping simulation method," J. Chem. Phys. **124**, 044109 (2006).

[38] Y. Cao, D. T. Gillespie, and L. R. Petzold, "The slow-scale stochastic simulation algorithm," J. Chem. Phys. **122**, 014116 (2005).

[39] E. L. Haseltine and J. B. Rawlings, "Approximate simulation of coupled fast and slow reactions for stochastic chemical kinetics," J. Chem. Phys. **117**, 6959–6969 (2002).

[40] D. T. Gillespie, "The chemical Langevin equation," J. Chem. Phys. **113**, 297–306 (2000).

[41] D. Bandak, N. Goldenfeld, A. A. Mailybaev, and G. Eyink, "Dissipation- range fluid turbulence and thermal noise," Phys. Rev. E **105**, 065113 (2022).

[42] J. B. Bell, A. Nonaka, A. L. Garcia, and G. Eyink, "Thermal fluctuations in the dissipation range of homogeneous isotropic turbulence," J. Fluid Mech. **939**, A12 (2022).

[43] K. Sreenivasan, "Possible effects of small-scale intermittency in turbulent reacting flows," Flow, Turbul. Combust. **72**, 115–131 (2004).

[44] N. Swaminathan and N. Chakraborty, "Scalar fluctuation and its dissipation in turbulent reacting flows," Phys. Fluids **33**, 015121 (2021).

12 April 2024 07:53:06